International Journal of Engineering Trends and Technology
ISSN: 2231 – 5381 / https://doi.org/10.14445/22315381/IJETT-V71I3P228

Volume 71 Issue 3, 276-281, March 2023
© 2023 Seventh Sense Research Group®

Original Article

Thermodynamics Study of Copper Recovery from Waste LFP (Lithium Iron Phosphate Battery)

Jong-deok Lim[1], Hyoun-Jong Kim[1], Jei-Pil Wang[1,2*]

[1]*Department of Metallurgical Engineering, Pukyong National University, Busan, Republic of Korea*
[2]*Division of Convergence Materials Engineering, Department of Metallurgical Engineering, Department of Marine Convergence Design Engineering (Advanced Materials Engineering), Pukyong National University, Busan, Republic of Korea*

[1,2*]*Corresponding Author : jpwang@pknu.ac.kr*

Received: 06 January 2022 Revised: 17 February 2023 Accepted: 20 March 2023 Published: 25 March 2023

Abstract *- In this study, a thermodynamic investigation was conducted to select a slag system capable of dry reduction treatment of Cu through the analysis of waste LFP batteries. Through this, the possibility of Cu recovery was reviewed. To remove C in the waste LFP battery, C was removed from the waste LFP battery in an O_2 atmosphere at 800 ° C for 2 hr. As a result of analyzing components, 42.25% of Cu and 39.52% of Fe were detected. First, Cu was separated and recovered in a matte form. After that, a thermodynamics review of the dry refining process was conducted to turn Fe in the slag into FeO for the low-carbon Fe reduction process. Therefore, FeO-SiO_2-Al_2O_3 was selected as the slag system, and through this, the possibility of manufacturing Cu in the waste LFP battery as matte using Factsage8.2.*

Keywords *- LFP battery, Molten reduction, Slag system, Cu recovery, Factsage.*

1. Introduction

In recent years, the size of the secondary battery industry has been greatly growing due to the rapid growth of electric vehicles and ESS. The lithium secondary battery market size in 2030 is expected to grow 17 times compared to 2019, and the price of raw materials is also expected to soar. In response to this trend, studies on increasing performance, such as the capacity and voltage of secondary batteries, have been actively conducted, and rapid development has been achieved. However, due to the structural characteristics of the secondary battery, the lifespan of the secondary battery is still about 10 years. Therefore, the explosively increasing size of the secondary battery industry will eventually generate a large amount of waste batteries in the future, and the recovery of valuable metals from waste batteries will be a key to the realization of a sustainable future society. [1,3,5,7]

The LFP battery, one of the representative lithium-ion batteries, is composed of cathode material, a cathode material, a separator, an electrolyte, etc., and is made using lithium iron phosphate ($LiFePO_4$), an olivine structure with high stability by replacing cobalt with iron phosphate in the existing layered lithium cobalt oxide (LCO) battery. Due to these structural characteristics of the cathode material, it has fewer disadvantages than lithium batteries in terms of short lifespan and risk of ignition/explosion. The price is low because iron is used instead of cobalt, an expensive raw material. Due to these comparative advantages, the market share of NCM/NCA is dominant until the present time, but the market share of LFP will increase significantly in the future. From the late 2020s, the lithium battery using lithium iron phosphate as a cathode material is expected to emerge as the No. 1 in terms of market share.[8]

In particular, the negative electrode uses a high-purity copper foil as a negative electrode plate and is coated with high-purity carbon. Although high-purity copper in these batteries is a valuable metal, studies have seldom been conducted on recycling technology, particularly Cu recovery through dry melting reduction refining.

The iron ore is largely divided into hematite (Fe_2O_3) and magnetite (Fe_3O_4). Hematite reacts with carbon monoxide generated from burning coke to produce carbon dioxide and magnetite, whereas magnetite reacts with carbon monoxide to produce carbon dioxide and iron. The chemical formulas (1) and (2) are expressed as flows:

$$3Fe2O3 + CO = 2Fe3O4 + CO2 \quad (1)$$

$$Fe3O4 + 4CO = 3Fe + 4CO2 \quad (2)$$

In the above reaction equation, hematite (Fe_2O_3) and magnetite (Fe_3O_4) require relatively more reducing agents

This is an open access article under the CC BY-NC-ND license (http://creativecommons.org/licenses/by-nc-nd/4.0/)

since they have a higher oxidation number than iron monoxide (FeO). Therefore, when Fe is reduced, more carbon dioxide is emitted than iron monoxide (FeO). When Fe and Cu are separated in the recycling process of the waste LFP battery if the slag is formed as FeO, the amount of reducing agent used in the Fe reduction process is expected to be further reduced.

In this study, based on the components and contents of the waste LFP batteries analyzed, a slag system was selected to recover copper, a valuable metal, through dry melting reduction treatment technology and, in particular, the SiO_2-FeO-Al_2O_3 system, which turns the iron component in the LFP battery into FeO slag, was reviewed through Factsage8.2, a thermodynamic analysis program.

2. Materials and Methods

CATL, a battery manufacturer in China, generated the waste LFP battery used in this study. First, the entire waste LFP was uniformly shredded using a shredder for component analysis, and the shape was expressed in Figure 1. In addition, since the waste battery that had passed through the shredder contained a large amount of Al case and PP film, which are components of the battery, the Al case and film were removed through a 4mm size sieve classification. After classification, the components of the waste LFP battery were analyzed by C/S.

Since the carbon component in the sample reduces iron (Fe) among the cathode material components in the battery during the dry melting reduction process, carbon was first removed to manufacture high-purity Cu matte. For the carbon removal process, to induce the reaction of Equation (3) below, 100g of screened and classified waste LFP battery sample was tested by injecting O_2 gas at 800°C for 2 hr using an atmosphere box furnace and to determine an appropriate amount of oxygen equivalent, three-stage experiments were conducted under the conditions expressed in Table 1.

Fig. 1 The shape of waste LFP battery that has passed through a shredder

Table 1. Conditions of the carbon removal experiment process

	O_2 (e.q)	O_2 input(L)	O_2 input(mm/min)
Stage 1	1.0	27.16	226
Stage 2	1.5	40.74	340
Stage 3	2.1	57.03	475

$$2C + O2 = 2CO \quad (3)$$

To examine the possibility of dry melting reduction treatment for the waste LFP battery debris, the phase equilibrium of slag was calculated and reviewed using the thermodynamics calculation program Factsage8.2, and the separation characteristics of Cu matte and slag were also calculated and reviewed by calculating viscosity.

Figure 2 below is the equilibrium diagram between Fe-FeO-Fe_3O_4 according to the oxygen distribution pressure. Among the components in the slag, FeO is precipitated as Fe_3O_4 and Fe_2O_3 phases at high oxygen distribution pressures, so it is necessary to maintain the FeO phase using an oxygen distribution pressure between the equilibrium oxygen distribution pressures of the reaction equation (4) and (5) below. Therefore, Factsage8.2 was used to calculate the appropriate equilibrium oxygen distribution pressure, and the distribution pressure was maintained by injecting CO/CO_2 mixed gas using an MFC (Mass Flow Controller).

$$Fe(l)1/2O2(g) = FeO(l) \quad (4)$$

$$FeO(l) + 1/2O2(g) = Fe3O4(l) \quad (5)$$

3. Result and Discussion

3.1. Screening and Classification Experiment of Waste LFP Battery Shreds

In general, graphite, an anode material used in the battery manufacturing process, is coated on a copper anode plate with ultra-high purity, serving as a structural material for lithium during charging/discharging. Figure 3 below shows the shape of the sample generated after screening and classifying LFP battery shreds using a 4mm sieve. As shown in the figure, even after screening classification, among the materials constituting the battery, PP film is included together, and a large amount of graphite anode material applied to the anode plate is also included.

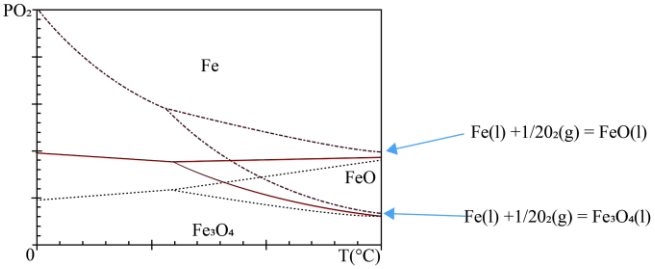

Fig. 2 Diagram of Fe-FeO-Fe_3O_4 according to the oxygen distribution pressure

Fig. 3 Photo of the waste LFP battery shreds after screening and classification

In the Table. 3 below, the results of the C/S analysis of waste LFP battery shreds are listed. A large amount of the negative electrode material applied to the copper negative plate was mixed, and the content was calculated as 29.1 (wt%).

Table 2. Result of CS analysis after screening and classification of waste LFP battery shreds

Element	Weight(%)
C	29.1

3.2. Carbon Removal Process after Screening A\and Classification

Table 2 below shows the results of the C/S analysis after removing the carbon component from the waste LFP battery through dry heat treatment by oxygen equivalent. When an excessive amount of oxygen is added to the carbon removal process, FeO components can turn to Fe_3O_4 and Fe_2O_3. Therefore, an appropriate amount of oxygen must be added to remove only carbon. The appropriate oxygen equivalent measured through the experiment was confirmed as 2.1 (e.q). In addition, after carbon removal, the components were analyzed through XRF inspection, and the results are listed in Table 3 below.

Table 3. Results of C/S analysis after carbon component removal by oxygen equivalent

	O_2 (e.q)	C/S analysis result (C. wt%)
Stage 1	1.0	8.232
Stage 2	1.5	3.651
Stage 3	2.1	0.190

Table 4. Result of XRF analysis of waste LFP battery after the carbon removal process

Element	Weight%
Cu	42.25
Fe	39.52
P	13.03
Al	2.84
Ni	0.89
S	0.55
Co	0.38
Cr	0.26
Si	0.24

3.3. Thermodynamics Review of Oxide Slag

Most of the waste battery samples used in this study consisted of 42.25% copper and 39.52% Fe. Through this, the highest density Cu(8.96g/cm^3) must be recovered in the form of matte, and Fe must be oxidized to the form of FeO to recover Cu from the iron component. In general, since copper used as a negative electrode in a waste battery exists as a high-purity copper foil, it can be recovered as Cu matte when an appropriate oxygen distribution pressure is maintained. However, the iron component exists in the form of LFP ($LiFePO_4$) in the positive electrode material. Therefore, Fe needs to be collected in slag in the form of oxides and removed. In addition, since lithium with a low boiling point volatilizes at high temperatures, it can be removed during the dry melting reduction process. Therefore, after volatilizing Li through the high-temperature dry melting reduction process of the waste LFP battery from which carbon was removed, the process of recovering the high-density copper foil in the form of matte by turning the Fe component into FeO was reviewed through thermodynamics analysis.

Based on the activity according to the FeO content in the slag calculated through Factsage8.2, the optimal oxygen distribution pressure at which FeO is well maintained was calculated, and the activity of each component was expressed in Table. 4 below. In addition, since the slag must be in a molten state for phase separation between the reduced metal and the slag, the lower the melting point of the slag, the more convenient the operation. In this study, to remove FeO as $2FeO\text{-}SiO_2$ (Fayalite) phase by adding SiO_2 as a slag composition to remove iron in Cu, $SiO_2\text{-}FeO\text{-}Al_2O_3$ slag system was reviewed.

Since the Al component analyzed in the waste LFP battery from which the carbon component has been removed exhibits significant oxidizing properties, it quickly forms an Al2O3 oxide film with a very small amount of oxygen.[9,10] In addition, the content of each component of the ternary slag system can be adjusted by calculating the Al component as the Al_2O_3 phase. Therefore, it can be seen that the $SiO_2\text{-}FeO\text{-}Al_2O_3$ slag phase is well maintained only by adding the SiO_2 component.

Figure 4 below shows the ternary phase diagram of $SiO_2\text{-}FeO\text{-}Al_2O$ between 1153°C and 2053°C was calculated using Factsage8.2. In the 1200°C section, it was found that Fe_2SiO_4 (Fayalite) was formed between F/S = 1.7 and 3.11, indicating it would be good to keep the target slag composition between F/S = 1.7 and 3.11.

Since the fluidity of slag is largely related to viscosity, the lower the fluidity, the better the separation between the matte and the slag, resulting in better properties. The viscosity of slag is highly dependent on the temperature and the content of acid/basic components in the slag.

Table 5. Component activity calculation by slag composition and temperature through Factsage8.2

(wt%)	SiO_2	FeO	Al_2O_3	FeO	SiO_2	Al_2O_3
1200˚C	37.38	59.77	2.84	3.1686E-01	8.1359E-01	4.4771E-04
1200˚C	32.38	64.77	2.84	4.4272E-01	4.9381E-01	6.2310E-04
1200˚C	27.38	69.77	2.84	5.5693E-01	3.1196E-01	1.0201E-03
1200˚C	22.38	74.77	2.84	6.6069E-01	2.0185E-01	1.4182E-03
1250˚C	37.38	59.77	2.84	3.0776E-01	8.3502E-01	4.1400E-04
1250˚C	32.38	64.77	2.84	4.5214E-01	4.7422E-01	6.7326E-04
1250˚C	27.38	69.77	2.84	5.6455E-01	3.0440E-01	1.0652E-03
1250˚C	22.38	74.77	2.84	6.6654E-01	1.9959E-01	1.4412E-03
1300˚C	37.38	59.77	2.84	2.9856E-01	8.5558E-01	3.7968E-04
1300˚C	32.38	64.77	2.84	4.6110E-01	4.5662E-01	7.2377E-04
1300˚C	27.38	69.77	2.84	5.7165E-01	2.9760E-01	1.1088E-03
1300˚C	22.38	74.77	2.84	6.7184E-01	1.9763E-01	1.4627E-03
1350˚C	37.38	59.77	2.84	2.8923E-01	8.7532E-01	3.4472E-04
1350˚C	32.38	64.77	2.84	4.6964E-01	4.4074E-01	7.7450E-04
1350˚C	27.38	69.77	2.84	5.7829E-01	2.9144E-01	1.1509E-03
1350˚C	22.38	74.77	2.84	6.7667E-01	1.9589E-01	1.4830E-03
1400˚C	37.38	59.77	2.84	2.7972E-01	8.9431E-01	3.0914E-04
1400˚C	32.38	64.77	2.84	4.7779E-01	4.2633E-01	8.2533E-04
1400˚C	27.38	69.77	2.84	5.8450E-01	2.8584E-01	1.1916E-03
1400˚C	22.38	74.77	2.84	6.8109E-01	1.9436E-01	1.5021E-03

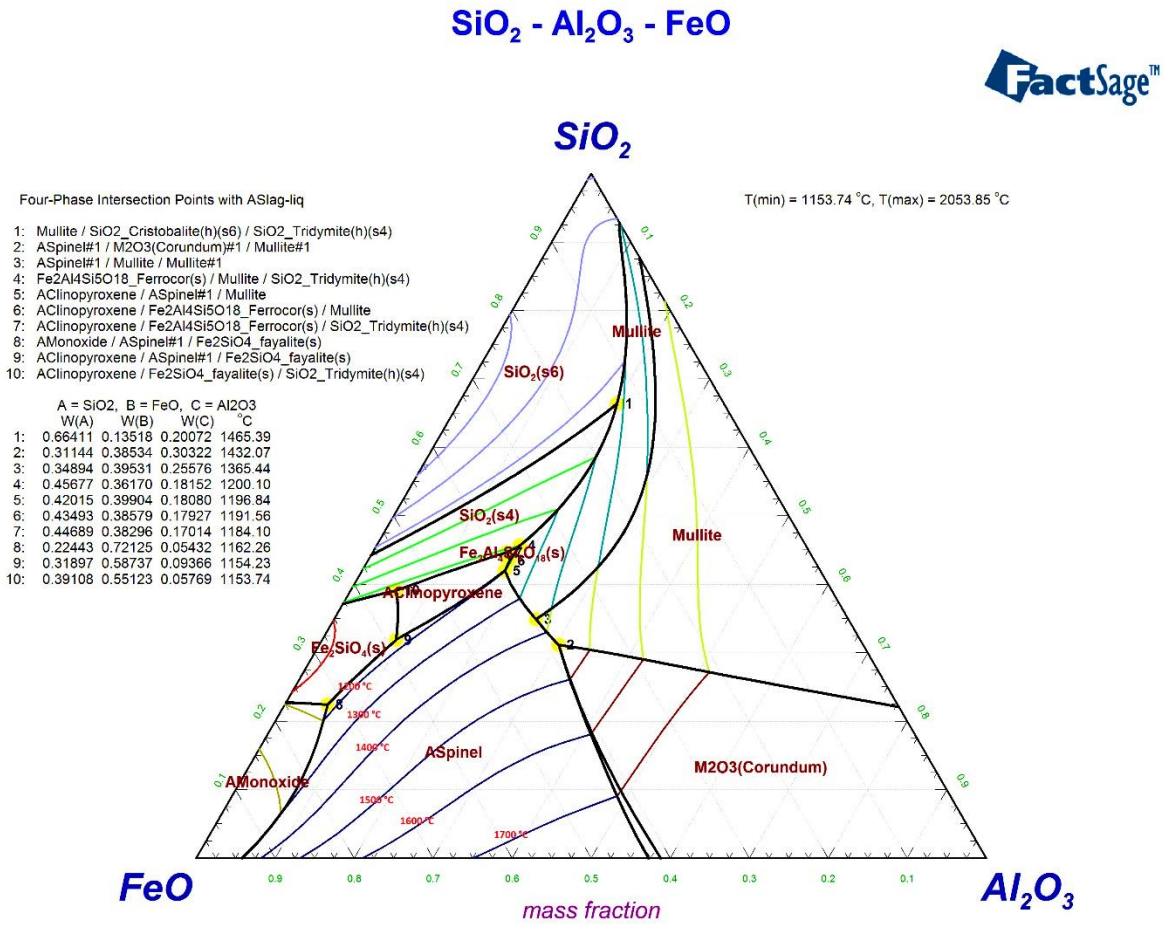

Fig. 4 SiO_2-Al_2O_3-FeO liquidus projection ternary phase diagram

Table 6. Changes in FeO and SiO_2 content and results of viscosity calculation results using Factsage8.2

	SiO_2(wt%)	FeO(wt%)	Al_2O_3(wt%)	Visc(poise)
1050˚C	37.38	59.77	2.84	7.086
1050˚C	32.38	64.77	2.84	3.174
1050˚C	27.38	69.77	2.84	1.667
1050˚C	22.38	74.77	2.84	0.983
1100˚C	37.38	59.77	2.84	4.996
1100˚C	32.38	64.77	2.84	2.335
1100˚C	27.38	69.77	2.84	1.265
1100˚C	22.38	74.77	2.84	0.764
1150˚C	37.38	59.77	2.84	3.616
1150˚C	32.38	64.77	2.84	1.756
1150˚C	27.38	69.77	2.84	0.978
1150˚C	22.38	74.77	2.84	0.604
1200˚C	37.38	59.77	2.84	2.678
1200˚C	32.38	64.77	2.84	1.347
1200˚C	27.38	69.77	2.84	0.770
1200˚C	22.38	74.77	2.84	0.486
1250˚C	37.38	59.77	2.84	2.025
1250˚C	32.38	64.77	2.84	1.052
1250˚C	27.38	69.77	2.84	0.616
1250˚C	22.38	74.77	2.84	0.396
1300˚C	37.38	59.77	2.84	1.561
1300˚C	32.38	64.77	2.84	0.835
1300˚C	27.38	69.77	2.84	0.500
1300˚C	22.38	74.77	2.84	0.327
1350˚C	37.38	59.77	2.84	1.223
1350˚C	32.38	64.77	2.84	0.672
1350˚C	27.38	69.77	2.84	0.411
1350˚C	22.38	74.77	2.84	0.274
1400˚C	37.38	59.77	2.84	0.973
1400˚C	32.38	64.77	2.84	0.548
1400˚C	27.38	69.77	2.84	0.342
1400˚C	22.38	74.77	2.84	0.231

Therefore, the viscosity was calculated according to the F/S ratio and temperature using the Factsage8.2 program, and the results are listed in Table 5 below. Since the content of FeO in the slag increased and the temperature of the slag increased, the viscosity tended to decrease, and generally, low viscosity values were calculated above 1200°C. Therefore, when the operating temperature was maintained above the melting point of the slag, the possibility of separating and recovering Cu and Fe components through the dry melting reduction process was confirmed.

4. Conclusion

In this study, to separate and recover the copper foil used as a negative electrode from the waste LFP battery through the dry melting reduction process, the optimal slag composition and operating temperature were investigated using Factsage8.2, a thermodynamic analysis program, and conclusions were obtained as follows:

1. The sample used in this study was recovered by screening and classifying the waste LFP batteries using a shredder and a 4mm sieve, and as a result of C/S analysis, 29.1% of carbon was observed.
2. Since the sample contained a large amount of carbon, the carbon was removed. When the oxygen equivalent was 2.1 (e.q), most of the carbon was removed, and as a result of C/S analysis, the carbon content was 0.190%.
3. The contents of Cu and Fe in the waste LFP battery from which carbon components were removed were found to be 42.25% and 39.52%, respectively. For the slag system for separating Cu and Fe, SiO_2-FeO-Al_2O_3 ternary phase system was selected because it can generate Fe_2SiO_4 (Fayalite) and remove Fe components. As a result of predicting it through liquidus projection calculation, it was found that Fe_2SiO_4 (Fayalite) was generated between F/S (FeO/SiO_2) = 1.70 ~ 3.11.

4. In the SiO_2-FeO-Al_2O_3 ternary phase system, the viscosity of slag was confirmed when the F/S ratio was 1.59, 2.00, 2.54, and 3.34, respectively, and when the temperature was from 1050°C to 1400°C, respectively. As a result, it was confirmed that the viscosity tended to decrease as the content of the FeO component and the temperature increased. When the slag temperature was 1200 ° C or higher, a generally good viscosity was calculated at a level of 1.347 (poise) or less.

Acknowledgments

This work was supported by the Korea Institute of Energy Technology Evaluation and Planning(KETEP) grant funded by the Korean government(MOTIE) (G032649311, Development of carbon-reducing battery raw material technology from waste lithium iron phosphate (LFP) batteries)

References

[1] " 2022 Global Outlook for Expansion of LIB Production Lines (~2030)," SNE Research, 2022. [Publisher link]

[2] Hyun-Jong Kim, Jong-Min Jeong, and Jei-Pil Wang, "A Study to Recover Si and Ag from Solar Cells and PV Ribbons by Utilizing Acid Solutions," *International Journal of Engineering Trends and Technology*, vol. 71, no. 1, pp. 222-233, 2023. [CrossRef] [Publisher link]

[3] Pratima Meshram, B.D. Pandey, and T.R. Mankhand, "Extraction of Lithium from Primary and Secondary Sources by Pre-treatment, Leaching and Separation: A Comprehensive Review," *Hydrometallurgy*, vol. 150, pp. 192-208, 2014. [CrossRef] [Google Scholar] [Publisher link]

[4] Bakhodir Abdullayev et al., "Lithium Recovery from Water Resources by Membrane and Adsorption Methods," *International Journal of Engineering Trends and Technology*, vol. 70, no. 9, pp. 319-329, 2022. [CrossRef] [Google Scholar] [Publisher link]

[5] Xiaoxiao Zhang et al., "Toward Sustainable and Systematic Recycling of Spent Rechargeable Batteries," *Chemical Society Reviews*, vol. 47, pp. 7239-7302, 2018. [CrossRef] [Google Scholar] [Publisher link]

[6] Renuka Sahu, "Application of Phase Change Materials in Heat Recovery from Blast Furnace Slag," *SSRG International Journal of Mechanical Engineering*, vol. 4, no. 3, pp. 19-22, 2017. [CrossRef] [Google Scholar] [Publisher link]

[7] Benjamin Ballinger et al., "The Vulnerability of Electric Vehicle Deployment to Critical Mineral Supply," *Applied Energy*, vol. 255, pp. 113844, 2019. [CrossRef] [Google Scholar] [Publisher link]

[8] Export-Import Bank of Korea, Trends and Prospects of the Battery Material Mineral Market: Focusing on Lithium, Nickel, and Cobalt, 2022 Industry Insight – 2(2022) *PDCA12-70 data sheet*, OptoSpeedSA, Mezzovico, Switzerland.

[9] J. Padhye, V. Firoiu, and D. Towsley, "*A Stochastic Model of TCP Reno Congestion Avoidance and Control*," CMPSCI Technical Report 99-02, 1999.

[10] S. Gudic et al., "Cathodic Breakdown of Anodic oxide film on Al and Al–Sn alloys in NaCl solution," *Electrochimica Acta*, vol. 50, no. 28, pp. 5624-5632, 2005. [CrossRef] [Google Scholar] [Publisher link]

[11] Dong Chen et al., "Corrosion of Aluminium in the Aqueous Chemical Environment of a Loss-of-Coolant Accident at a Nuclear Power Plant," *Corrosion Science*, vol. 50, no. 4, pp. 1046-1057, 2008. [CrossRef] [Google Scholar] [Publisher link]

[12] Jens Breckling, *The Analysis of Directional Time Series: Applications to Wind Speed and Direction*, Lecture Notes in Statistics, vol. 61, no. 1, pp. 200-220, 1989. [Google Scholar] [Publisher link]